

A 2 Bit Reconfigurable Beam-Steering Antenna Array Using Phase Compensation

Xiuwen Tian and Lizhong Song*

Abstract—A 2 bit reconfigurable beam-steering antenna array using phase compensation is proposed, which consists of a 1 bit reconfigurable antenna and 90° digital phase shifter. The p-i-n diodes are soldered in the 2 bit element to realize 2 bit phase shift. Due to the 2 bit phase quantization error, a fixed compensation phase is added to each array element to reduce sidelobe level. A 2 bit reconfigurable antenna array with 1×8 elements shows that the sidelobe levels of the scanning-beams are less than -6.2 dB. At the same time, simulated results also show that the antenna can steer beam direction from -48° to 50° , and the beam gain fluctuation is less than 2.2 dB. A prototype is fabricated and tested. The proposed antenna can provide a novel idea to design a 2 bit reconfigurable beam-steering antenna array with a better beam-scanning performance in various applications.

1. INTRODUCTION

Reconfigurable antennas can dynamically scan beam, which has excellent features, such as low cost, simple fabrication process, simplified control logic, and low insertion loss. As it is well known, a phased array antenna needs expensive transmitting/receiving (T/R) modules to control the current amplitude and phase of each array element, so it has a higher cost. Thus, reconfigurable antennas are an attractive alternative to the conventional phased array antenna. Reconfigurable antennas have been greatly developed for beam-steering recently.

Reconfigurable antennas can be categorized into two types, according to integrated varactor diodes and p-i-n diodes, which are analog reconfigurable antennas [1] and digital reconfigurable antennas [2, 3]. According to different designing approaches, reconfigurable antennas can also be divided to reconfigurable reflectarray antenna (RRA) [4–6], reconfigurable transmitarray antenna (RTA) [7–9], and reconfigurable metasurface [10, 11]. Reconfigurable transmitarray antenna integrating varactor diodes can continuously tune phases, which needs a continuous analog voltage [12, 13]. Each RTA element needs many voltage values which would complicate beam controlling circuit. In order to obtain a simple beam control circuit, p-i-n diode is used to replace varactor diode, which can obtain a discrete phase. Compared to RTA, RRA has an aperture occlusion problem [14, 15]. The element design is vital to RRA and RTA, which can decide the RRA and RTA functions [16]. For broadband RTA and RRA design, the broadband polarization rotation element and slotted metallic square patch can be utilized to design wideband RTA [7] and RRA [6], respectively. By designing RTA element, RTA can transform the incident linear polarization (LP) wave into outgoing circularly polarized (CP) wave [13]. Due to the 1 bit RTA and RRA having a high sidelobe level and low aperture efficiency, a 2 bit RTA element [17–19] and RRA element [20] are designed. However, the RTA and RRA have a high profile that limits their application in many low-profile scenarios.

Metasurface and metamaterial can be utilized to design low-profile reconfigurable antenna. A programmable metasurface based on substrate-integrated waveguide can steer beam direction from

Received 15 August 2022, Accepted 11 October 2022, Scheduled 1 November 2022

* Corresponding author: Lizhong Song (songlz@hit.edu.cn).

The authors are with the School of Electronics and Information Engineering, Harbin Institute of Technology, Harbin 150001, China.

-25° to 33° [21]. On the other hand, with p-i-n diode states switching, the phase constant β of the metamaterial antenna can switch from β_0 to β_1 . By controlling the phase constant β , the metamaterial antenna array can achieve beam-scanning from -30° to 30° [22]. For frequency selective surface (FSS) design, a reconfigurable FSS structure is divided into four equal sections. By controlling the states of the p-i-n diodes on different sections, the proposed partially reflective surface (PRS) antenna can scan beam from -22° to 22° [23]. However, the reconfigurable antenna array based on the Metasurface and metamaterial has a limited scanning angle range. A circularly polarized 2 bit reconfigurable antenna array can steer beam direction from -49° to 49° , which has a simple beam-steering circuit and low-profile [24]. Due to the existence of 2 bit phase quantization error, compared with the conventional phased arrays, a linearly polarized 2 bit reconfigurable beam-steering antenna array has a higher sidelobe level [25].

To reduce the sidelobe level of the linearly polarized 2 bit reconfigurable beam-steering antenna array, this paper adopts a phase compensation method. The array element is composed of a 1 bit reconfigurable antenna and 90° digital phase shifter. For phase compensation, fixed compensation phases are added to each array element. Simulated results show that the proposed antenna can steer beam direction from -48° to 50° , and the sidelobe levels are less than -6.2 dB. This paper is organized as follows. To begin with, a 1 bit reconfigurable antenna, 90° digital phase shifter, and 2 bit reconfigurable antenna are shown in Section 2, and the working principles and design process are described in details. Then, Section 3 analyzes the beam-steering principle of the 2 bit reconfigurable antenna array, proposes a phase compensation method, and designs a 2 bit reconfigurable beam-steering antenna array using phase compensation. Section 4 presents the experiment and analyzes the measured results in details. Finally, Section 5 summarizes this work.

2. DESIGN AND ANALYSIS OF 2 BIT RECONFIGURABLE ANTENNA

2.1. 1 Bit Reconfigurable Antenna Design and Analysis

The geometry of the proposed 1 bit reconfigurable antenna is shown in Figure 1. The symmetric dipole elements are printed on a F4BTM-1/2 dielectric substrate ($\epsilon_r = 4.4$, $\tan \delta = 0.0025$) with the thickness of 3 mm. Two Infineon-BAR5002VH6327 p-i-n diodes are integrated on the symmetric dipole elements, respectively, which are equivalent to a series of RLC elements: $R_p = 3 \Omega$, $L_p = 0.6$ nH for ON state and $C_p = 0.15$ pF, $L_p = 0.6$ nH for OFF state. To control the p-i-n diodes state, open-ended radial stubs are used to choke RF signal and connect DC bias voltage circuit. At the same time, the symmetrical open-ended radial stubs can keep the current symmetric distribution on dipole element. The DC bias

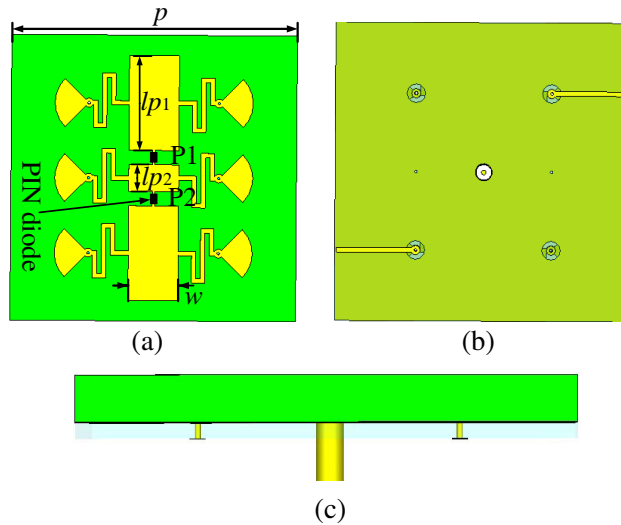


Figure 1. Geometry of the 1-bit reconfigurable antenna. (a) Top view. (b) Bottom view. (c) Side view.

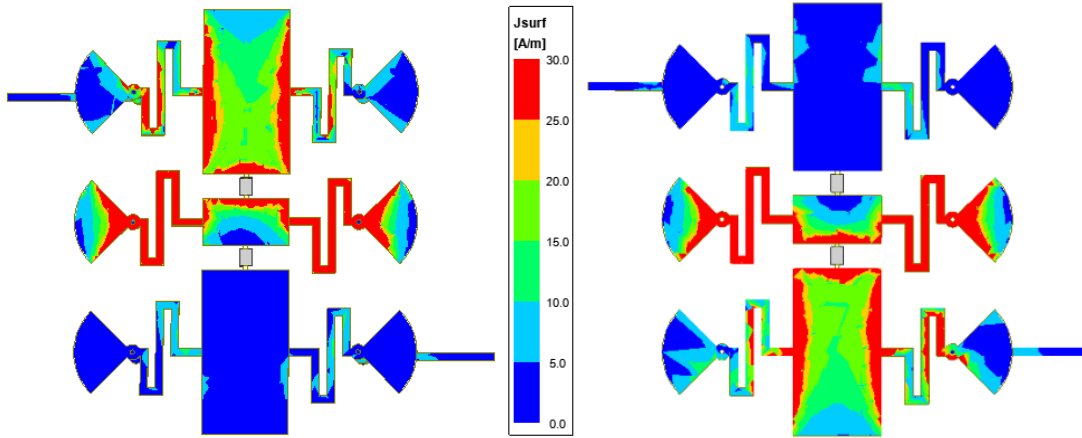


Figure 2. Current distribution of the 1 bit reconfigurable at state1 and state2.

Table 1. Pin diode state of the different phase shift states.

State	P1	P2	P3–P6	P7–P10
State1	OFF	ON		
State2	ON	OFF		
State3			ON	OFF
State4			OFF	ON
0°	ON	OFF	OFF	ON
90°	ON	OFF	ON	OFF
180°	OFF	ON	OFF	ON
270°	OFF	ON	ON	OFF

voltage circuits are printed on a layer of FR4 dielectric substrate with the thickness of 1 mm, which are placed under the ground plane. The DC bias voltage circuits and open-ended radial stubs are connected by metal vias. Two open-ended radial stubs in the middle of the antenna are used to connect ground plane, which can provide a low voltage for p-i-n diodes. A 50 Ω RF cable acts as a feeding line to connect the feeding node of the antenna. After optimization, the dimensions are: $lp1 = 10.6$ mm, $lp2 = 3$ mm, $p = 32$ mm, $w = 5.6$ mm.

The 1 bit reconfigurable antenna is simulated by using Ansys HFSS 2020. Figure 2 shows the simulated current distribution on the symmetric dipole elements. State1 and state2 are the two states of the p-i-n diodes, which are described in Table 1. It can be seen clearly that the current is transmitted from one side of the slot to another side by coupling. At the same time, the edge current amplitude of the slot is extremely low when the p-i-n diode in the slot is ON. The microstrip patch obtained energy by coupling and the slot with high current amplitude can radiate pattern to the upper half-space, and the other side microstrip patch and slot cannot radiate pattern. This current reversal phenomenon indicates that the radiation pattern of the 1 bit reconfigurable antenna can generate a 180° phase shift by switching p-i-n states. Figure 3 shows the simulated S -parameters and radiation pattern.

In Figure 3, at state1 and state2, the S_{11} and radiation pattern are stable. Within $S_{11} \leq -10$ dB, the simulated antenna working frequency bandwidth is 140 MHz from 5.19 GHz to 5.33 GHz. Figure 3(b) shows that the radiation pattern gain is 5.69 dB at 5.25 GHz, and the half-power beamwidth is 91° and 96°, respectively, in E -plane and H -plane. Figure 2 shows that the slot radiates most energy, and the distance between two symmetric slots is 4.6 mm. Because the two slots are close, in E -plane, the radiation patterns have a slight change with the p-i-n state switching in Figure 3.

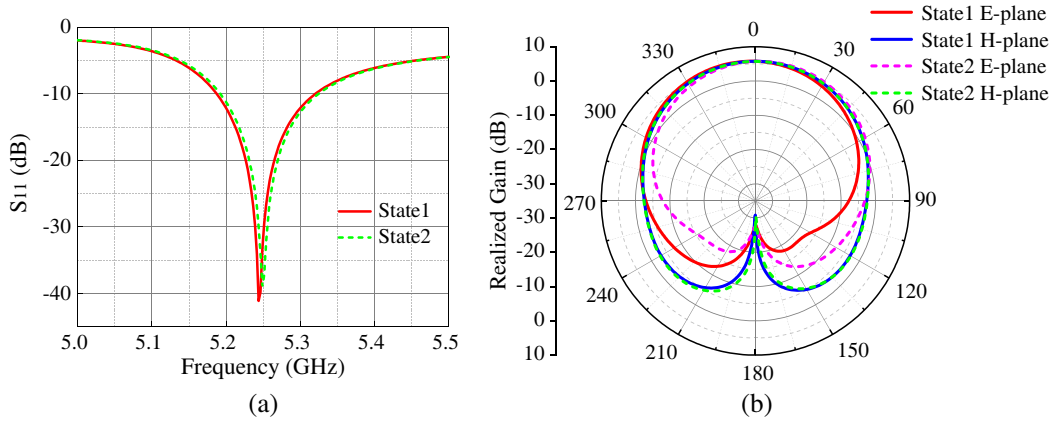


Figure 3. Simulated S -parameters and radiation pattern at state1 and state2. (a) S -parameters. (b) Radiation pattern.

2.2. Design and Analysis of 90° Digital Phase Shifter

The geometry of the proposed 90° digital phase shifter is shown in Figure 4. The phase shifter is composed of a two-layer dielectric substrate. The up-layer dielectric substrate is F₄B265 ($\epsilon_r = 2.65$, $\tan \delta = 0.001$) with the thickness of 2 mm, and down-layer dielectric substrate is FR4 ($\epsilon_r = 4.4$) with the thickness of 1 mm. Phase shifter circuit is printed on the top-surface of the up-layer dielectric substrate, and controlling circuit is printed on the bottom-surface of the down-layer dielectric substrate. The phase shifter circuit and controlling circuit are isolated by ground plane and connected by metal vias. Two open-ended radial stubs are used to choke RF signal and connect DC bias voltage circuit. The dimensions are optimized by Ansys HFSS 2020, which are $l_1 = 12.6$ mm, $l_2 = 10.2$ mm, $w_1 = 0.8$ mm, $w_2 = 2.6$ mm, $w_3 = 4.6$ mm. Two delay circuits can realize a different phase shift. By tuning the length of the delay circuit, the phase shifter can achieve a phase shift difference. To avoid the RF current on the one delay circuit flowing to the other delay circuit, two Infineon-BAR5002VH6327 p-i-n diodes are placed at the end of the delay circuit, which can provide a good isolated between two delay circuits.

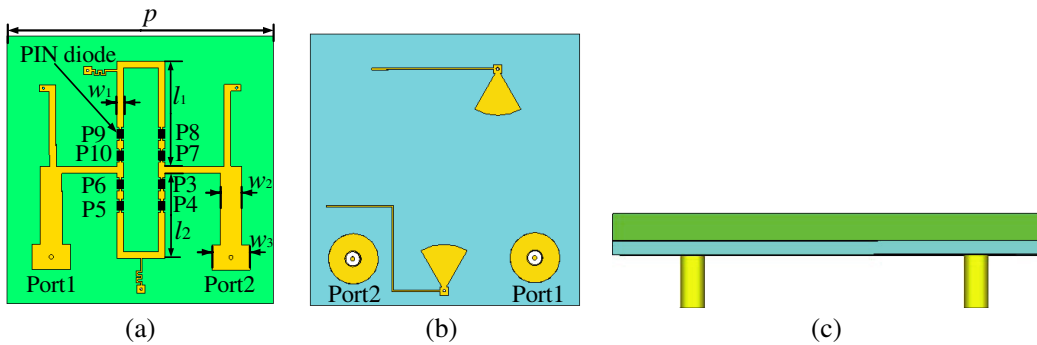


Figure 4. Geometry of the proposed 90° digital phase shifter. (a) Top view. (b) Bottom view. (c) Side view.

To obtain 90° phase shift, the p-i-n diodes are divided to state3 and state4 that are described in Table 1. At the two states, the current distributions are simulated, which are shown in Figure 5. In Figure 5, the current distributes on the delay circuit when the p-i-n diodes in the delay circuit are ON, and the current value is extremely low when the p-i-n diodes are OFF at state3. At state4, by energy coupling, there are a lower current distributed on the delay circuit with p-i-n OFF. This current distribution phenomenon indicates that the phase shift can be tuned by changing the length of the delay circuit. The transmission amplitude and phase shift are simulated, which are shown in Figure 6.

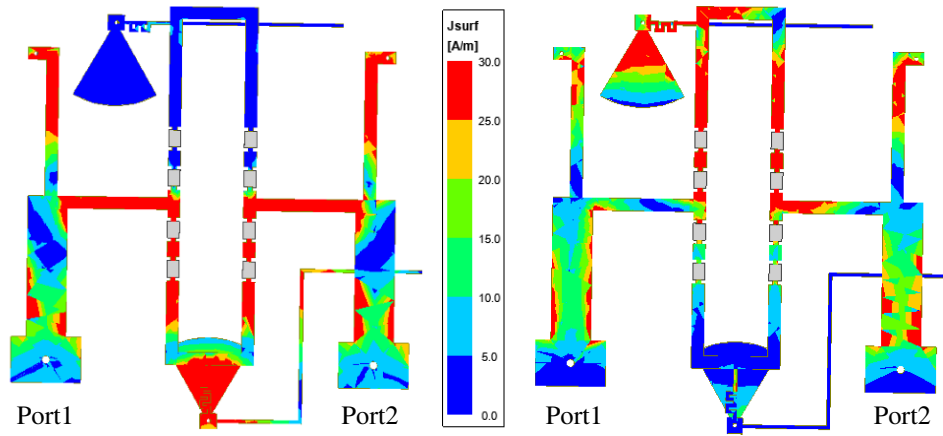


Figure 5. Current distribution of the 90° digital phase shifter at state3 and state4.

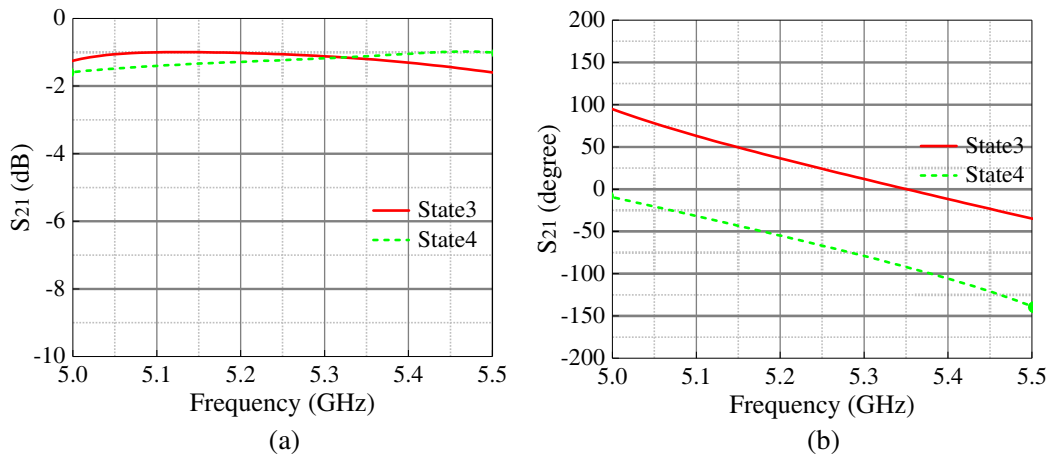


Figure 6. Simulated transmission magnitude and phase shift of the 90° digital phase shift. (a) Transmission magnitude. (b) Phase shift.

It can be clearly seen from Figure 6 that the simulated phase shift between state3 and state4 can reach $90^\circ \pm 5^\circ$ from 5.2 GHz to 5.4 GHz, and the transmission amplitude is less than -1.5 dB from 5.1 GHz to 5.4 GHz. At 5.25 GHz, the phase shift and transmission amplitude are 90° and -1.3 dB, respectively. Thus, the designed 90° digital phase shift has a good phase and transmission performance.

2.3. 2 Bit Reconfigurable Antenna

Figure 7 shows the proposed 2 bit reconfigurable antenna that is composed of a 1 bit reconfigurable antenna and a 90° digital phase shifter. It can be seen from Figure 7 that the 1 bit reconfigurable antenna and 90° digital phase shifter are connected by a bent RF cable. The height of the 2 bit reconfigurable antenna is 28 mm. The phase shifter can radiate pattern to the back of the 2 bit reconfigurable antenna, which will rise the back gain of the radiation pattern. A copper ground plane is adopted to reduce the back gain and improve the radiation pattern. The simulated results of the proposed 2 bit reconfigurable antenna are shown in Figure 8.

In Figure 8(a), the simulated S_{11} is less than -10 dB within the frequency bandwidth from 5.22 GHz to 5.37 GHz. At 5.25 GHz, S_{11} can reach -12 dB at different phase shift states. The frequency bandwidth of the S_{11} curve at 0° and 180° is greater than the S_{11} curve at 90° and 270° . The reason is that the two delay circuits of the 90° digital phase shifter have different impedance match states. Figure 8(b) shows

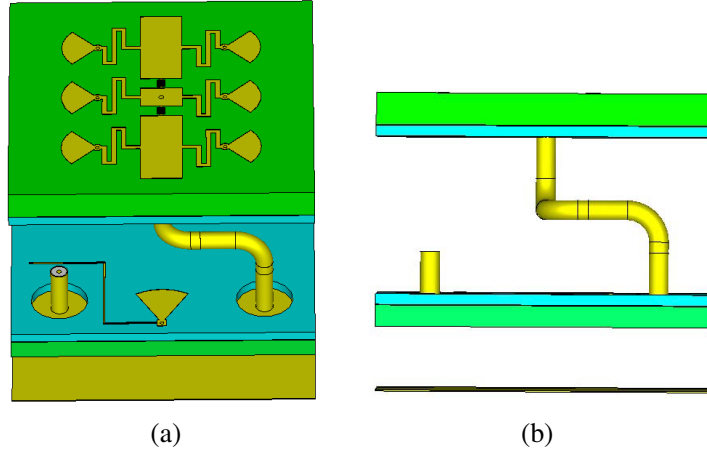


Figure 7. Geometry of the 2 bit reconfigurable antenna. (a) Top view. (b) Side view.

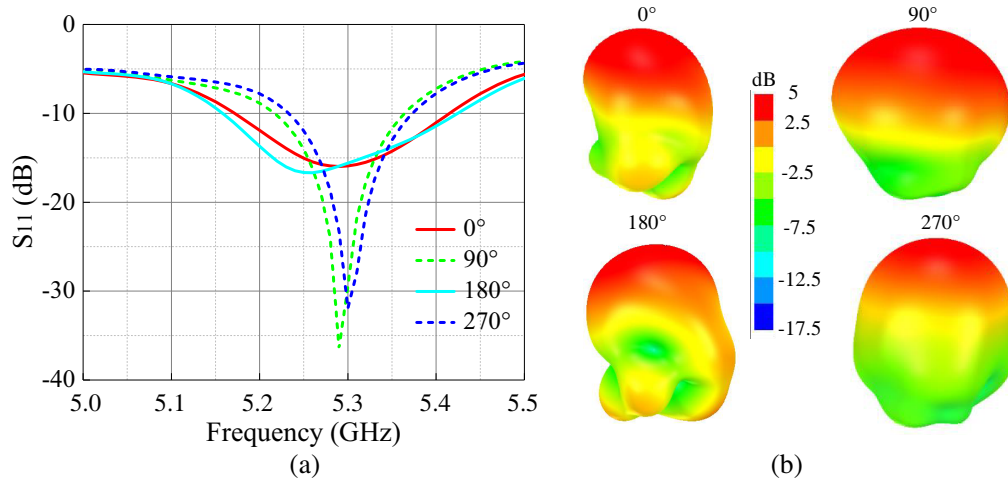


Figure 8. Simulated S -parameters and radiation pattern of the 2 bit reconfigurable antenna. (a) S -parameters. (b) Radiation pattern.

a three-dimensional radiation pattern at 2-bit phase shift states. Because the 0° and 180° phase states radiate more energy to the back half-space than the 90° and 270° , the radiation patterns at 90° and 270° are better than the radiation patterns at 0° and 180° . During beam-scanning, the risen sidelobe gain of the 2-bit reconfigurable antenna element has a little effect on the beam-scanning performance. The simulated radiation patterns clearly demonstrate that the proposed 2-bit reconfigurable antenna has a good radiation pattern performance.

3. 2 BIT RECONFIGURABLE BEAM-STEERING ANTENNA ARRAY USING PHASE COMPENSATION DESIGN

3.1. 2 Bit Reconfigurable Beam-Steering Antenna Array

Figure 9 shows the basic framework of the 2-bit reconfigurable beam-steering antenna array. The antenna array is composed of eight elements. Each element connects a 2-bit phase shifter that can provide 0° , 90° , 180° , and 270° phase states. A eight-way power divider is used to connect the array element. According to the phased array antenna theory [26], when the beam angle is θ , the excitation phase

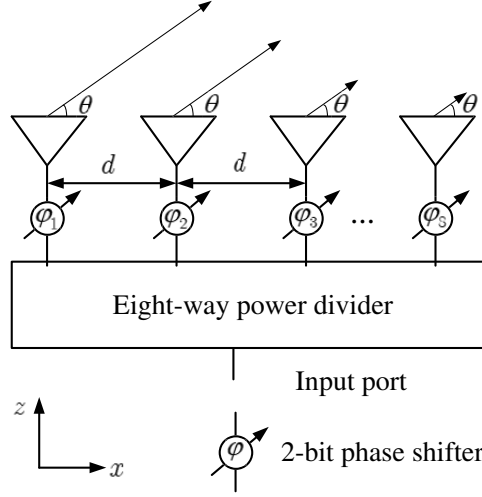


Figure 9. The framework of the 2 bit reconfigurable beam-steering antenna array.

difference $\Delta\phi$ between adjacent elements is

$$\Delta\phi = \frac{2\pi \sin(\theta)d}{\lambda_0} \tag{1}$$

d is the distance between adjacent elements, and λ_0 is the free space wavelength.

The excitation phase $\Delta\varphi_i$ for the i th element is

$$\Delta\varphi_i = (i - 1) \times \Delta\phi, \quad i = 1, 2, \dots, 8 \tag{2}$$

The phase range of $\Delta\varphi_i$ is from 0° to 360° . Because the 2 bit reconfigurable antenna has 0° , 90° , 180° , and 270° phase states, the excitation phase $\Delta\varphi_i$ is

$$\Delta\varphi_i = \begin{cases} 0^\circ, & \Delta\varphi_i \leq 45^\circ \text{ or } \Delta\varphi_i > 315^\circ \\ 90^\circ, & 45^\circ < \Delta\varphi_i \leq 135^\circ \\ 180^\circ, & 135^\circ < \Delta\varphi_i \leq 225^\circ \\ 270^\circ, & 225^\circ < \Delta\varphi_i \leq 315^\circ. \end{cases} \tag{3}$$

Formula (3) indicates that the maximum phase quantization error can reach 45° for the excitation phase $\Delta\varphi_i$ during beam-scanning. According to formulas (1), (2), and (3), the 2 bit reconfigurable antenna array can steer beam at desired direction. Ansys HFSS 2020 is used to simulate the beam-scanning performance. The beam-scanning performance of the 2 bit reconfigurable antenna array is shown in Figure 10 and Table 2.

In Table 2, with the beam-scanning angle increasing, the gain is gradually decreasing, and the gain loss is less than 2.5 dB within the beam angle range from -47° to 48° . Due to the scanning-beam having a symmetrical characteristic, the scanning-beam from 0° to -47° will be discussed. When the beam angle is from 0° to -30° , the sidelobe level is rapidly increasing from -12.5 dB to -5.7 dB. At the same time, the beam directions are -30° , -43° , and -47° with sidelobe levels of -5.7 dB, -5.0 dB, and -5.2 dB, respectively. Thus, the 2-bit reconfigurable antenna array has a stable beam gain and high sidelobe level during beam-scanning.

3.2. 2 Bit Reconfigurable Beam-Steering Antenna Array Using Phased Compensation

The main reason of high sidelobe level is the 2 bit phase quantization error. A phase compensation method is used to decrease the phase quantization error influence. Because the proposed antenna is symmetrical, the scanning-beam is also symmetrical about 0° in H -plane. To reduce calculation complexity, this paper selects the gradient phase of the four scanning-beams to calculate compensation phase, and the four scanning-beam angles are 0° , 15° , 30° , and 45° . According to formulas (1) and

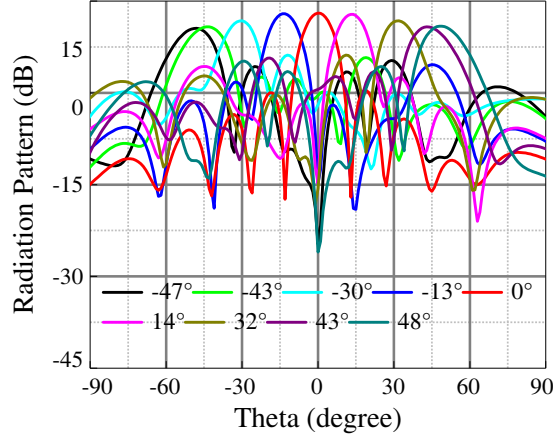


Figure 10. The beam-scanning performance of the 2 bit reconfigurable beam-steering antenna array.

Table 2. Beam-scanning performance of 2 bit reconfigurable beam-steering antenna array.

Scan Angle	Gain (dB)	Side Lobe Level (dB)
48°	10.9	-5.7
43°	10.7	-5.0
32°	11.7	-5.5
14°	12.8	-8.5
0°	13.0	-12.5
-13°	12.9	-8.3
-30°	11.8	-5.7
-43°	10.7	-5.0
-47°	10.5	-5.2

(2), $\Delta\phi_i$ of the four scanning-beams can be calculated at each element port. In fact, $\Delta\phi_i$ and the excitation phase provided from 2 bit element have a phase difference during beam-scanning. Based on $\Delta\phi_i$ of the four scanning-beam angles, the compensation phase can be obtained by providing the minimum phase difference for each element. However, for each element, when there is a contradiction between different scanning angles, the compensation phase of the larger scanning angle would be selected. According to the phase difference at different beam angles, the compensation phase of each element can be calculated. The calculated compensation phase $\Delta\phi_i$ is added to the i th array element. By adding the fixed compensation phase, the excitation phase of the i th array element $\Delta\varphi_i$ can be obtained as follows:

$$\Delta\varphi_i = \begin{cases} 0^\circ, & (\Delta\varphi_i + \Delta\phi_i) \leq 45^\circ \text{ or } (\Delta\varphi_i + \Delta\phi_i) > 315^\circ \\ 90^\circ, & 45^\circ < (\Delta\varphi_i + \Delta\phi_i) \leq 135^\circ \\ 180^\circ, & 135^\circ < (\Delta\varphi_i + \Delta\phi_i) \leq 225^\circ \\ 270^\circ, & 225^\circ < (\Delta\varphi_i + \Delta\phi_i) \leq 315^\circ. \end{cases} \quad (4)$$

The calculated compensation phase distribution of the 2-bit reconfigurable beam-steering antenna array are $0^\circ, 30^\circ, 17^\circ, 40^\circ, 40^\circ, 17^\circ, 30^\circ, \text{ and } 0^\circ$. By tuning the RF cables length of each array element, the fixed compensation phases can be applied to the array element. A 2 bit reconfigurable beam-steering antenna array with the compensation phase is designed, which is shown in Figure 11. The array size is $338 \text{ mm} \times 32 \text{ mm} \times 28 \text{ mm}$. The S -parameters and beam-scanning performance of the proposed 2 bit reconfigurable beam-steering antenna array are simulated, which are shown in Figure 12 and Figure 13, respectively.

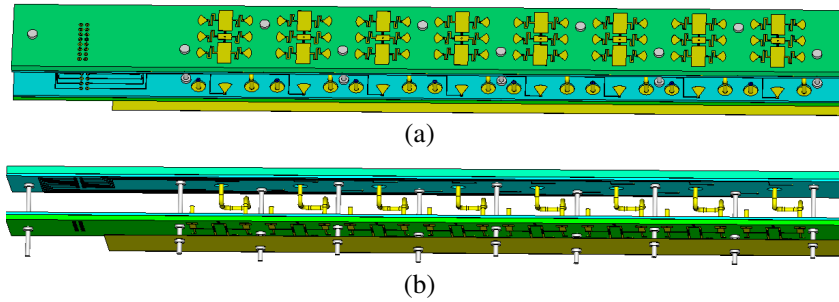


Figure 11. Geometry of the 2 bit reconfigurable beam-steering antenna array using phase compensation. (a) Top view. (b) Bottom view.

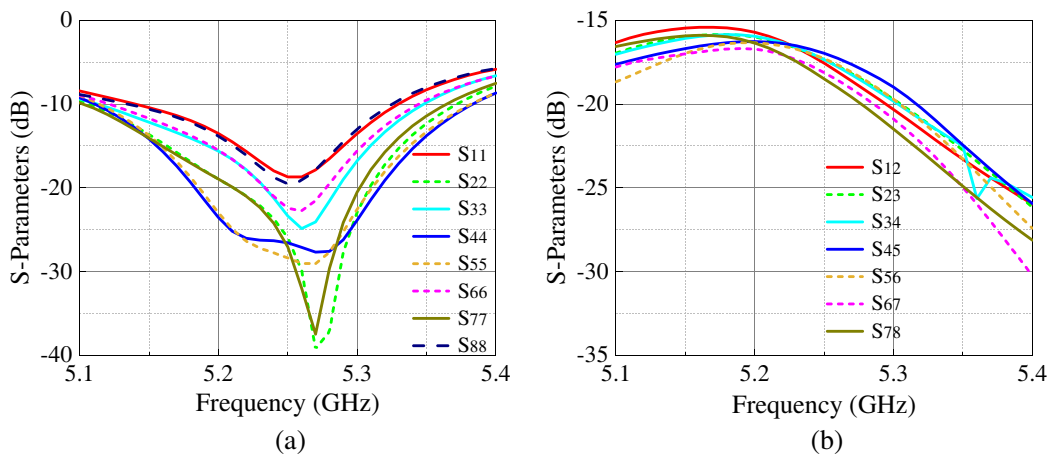


Figure 12. Simulated S -parameters of the 2 bit reconfigurable beam-steering antenna array using compensation phase. (a) Reflection coefficient. (b) Mutual coupling coefficient.

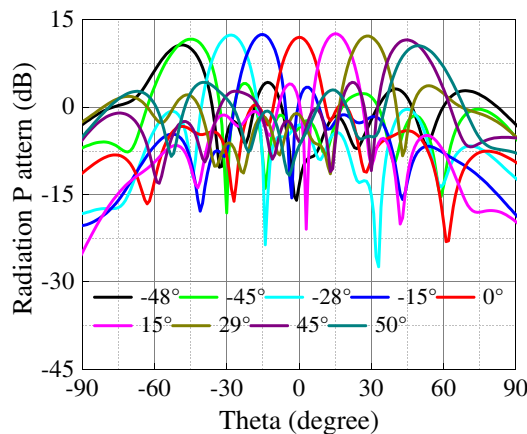


Figure 13. Simulated beam-scanning performance of the 2 bit reconfigurable beam-steering antenna array using phase compensation.

In Figure 12, the working frequency bandwidth of the antenna array is 200 MHz from 5.15 to 5.35 GHz, and the mutual coupling between two adjacent elements is smaller than -15 dB. Figure 13 shows that the proposed antenna array can scan beam from -48° to 50° at 5.25 GHz. The sidelobe level rises with the scanning-beam angle increasing. The key performance parameters of the scanning-beams are summarized in Table 3. Due to adopting a phase compensation method to the antenna array, the

Table 3. Beam-scanning performance of the 2 bit reconfigurable beam-steering antenna array using phase compensation.

Scan Angle	Gain (dB)	Side Lobe Level (dB)
50°	10.5	-6.2
45°	11.5	-7.3
29°	12.2	-8.5
15°	12.7	-8.7
0°	12.0	-11.3
-15°	12.5	-9.1
-28°	12.4	-8.7
-45°	11.7	-7.7
-48°	10.7	-6.4

-15°, 15°, -28°, and 29° beam gains are higher than the 0° beam gain. Compared with 0° beam, the gain loss is 1.3 dB and 1.5 dB for the -48° and 50° beams in H -plane, and the beam gain fluctuation is less than 2.2 dB with the beam direction from -48° to 50°. At the same time, the sidelobe levels are less than -6.2 dB. The antenna array can realize a wider angle beam-scanning with little gain fluctuation. Compared with Table 2, the gain decreases from 13.0 dB to 12.0 dB, and the sidelobe level increases from -12.5 dB to -11.3 dB at 0° beam. At the other beam angles, the sidelobe levels decrease, which are improved by using phase compensation. The simulated antenna array has an aperture efficiency of 50%. Therefore, by adding fixed compensation phase for each array element, the proposed 2 bit reconfigurable antenna array can obtain a better sidelobe level during beam-scanning.

4. FABRICATION AND EXPERIMENT

The proposed 2 bit reconfigurable antenna array is fabricated and measured, which is shown in Figure 14. As shown in Figure 14, a eight-way power divider adopts an RF cable to connect antenna array. Two digital control circuit boards with 384 output channels are used to control the 90° digital phase shifter and 1 bit reconfigurable antenna states, respectively. Each pin of the digital control circuit board can output DC voltage from 0 V to 3 V. The digital control circuit board connected to the phase shifter outputs 1.8 V/0 V DC voltage, and another digital control circuit board connected the 1 bit reconfigurable antenna outputs 0.9 V/0 V DC voltage.

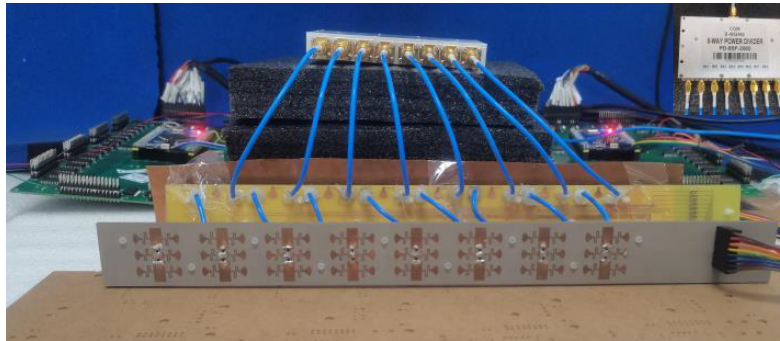


Figure 14. Photograph of the fabricated 2 bit reconfigurable beam-steering antenna array using phase compensation.

Figure 15(a) shows that the measured S_{11} curves become flat, and the frequency bandwidth becomes wider. The S_{11} curves at 90° and 270° become worse than the simulated ones, which is caused by the

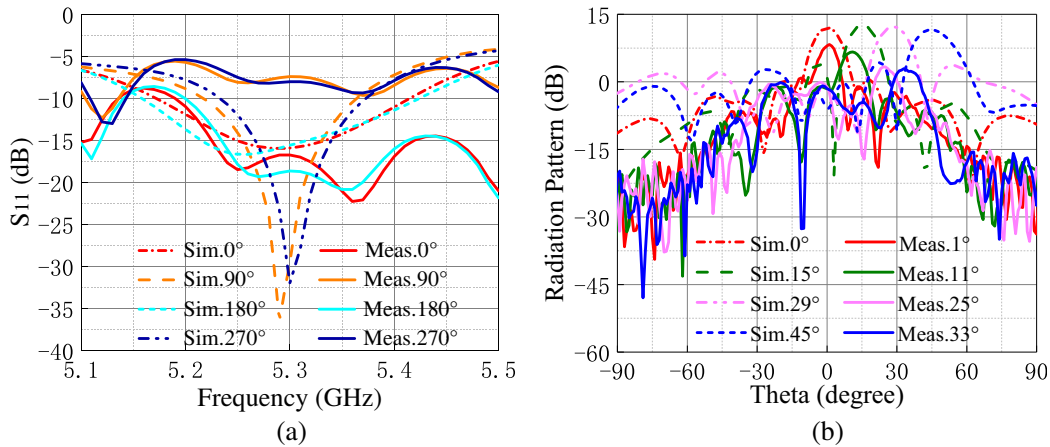


Figure 15. Measured S -parameters and beam-scanning performance. (a) S -parameters. (b) Radiation pattern.

fabrication and assembling error. In Figure 15(b), the main beam angle of the measured radiation patterns can reach 33°, which is smaller than the simulated ones, and the measured gains are 8.2 dB, 6.6 dB, 3.3 dB, and 2.9 dB at 1°, 11°, 25°, and 33°, respectively. The fabricated antenna array has an aperture efficiency of 20.9% at 1°. In fact, the p-i-n diodes have a insertion loss, and the insertion loss of the fabricated 90° phase shifter is greater than the simulated one. Those additional losses would cause the antenna array gain and aperture efficiency decreasing. Compared with the simulated beam gain, with the beam angle increasing, the measured beam gain is gradually decreasing. The fabricated 90° phase shifter has different impedance match states at 0° and 90°, which also generates a different insertion loss. The nonuniform insertion loss distributes on the antenna array during beam-scanning, which would reduce the beam-scanning range. With the scanning-beam angle increasing, the beam gain would decrease rapidly. The reasons for the unsatisfactory measured results include non-standard measured environment, fabrication error, assembling error, RF cable loss, and power divider loss.

In order to obtain a good performance in the future, multilayer circuit boards should adopt PCB pressing process, and the p-i-n diodes and RF cable should be precisely welded. The phase shifter should adopt a p-i-n diode with high isolation and low loss as a switch to reduce the p-i-n diode effect. The RF cable should have a low loss and stable transmission phase performance at working frequency. For the beam-scanning measurement, the proposed antenna array should be measured at a far-field anechoic chamber.

5. CONCLUSION

In this paper, a 2-bit reconfigurable beam-steering antenna array using phase compensation is proposed. The proposed antenna array adopts a 1-bit reconfigurable antenna and a 90° digital phase shifter to design a 2 bit reconfigurable element. The 1 bit reconfigurable antenna and 90° digital phase shifter are connected by an RF cable. A phase compensation method is used to improve the beam-scanning performance. By tuning the length of the RF cable for each array element, the array element can obtain a fixed compensation phase. By adding the compensation phase for each array element, the antenna array obtains a better sidelobe level. Simulated results show that the proposed antenna array can scan beam from -48° to 50° by controlling the p-i-n diodes states, and the beam gain fluctuation is less than 2.2 dB. For a 2 bit linear polarization reconfigurable antenna array, this paper adopts a phase compensation method to reduce the high sidelobe level caused by 2 bit phase quantization error, which can provide a novel method to enhance beam-scanning performance of the 2 bit reconfigurable antenna array in various applications.

ACKNOWLEDGMENT

This work is sponsored by the Foundation of the Key Laboratory of Science and Technology for National Defense (6142401200401), the Science Foundation of Aeronautics of China (20200018037001), the Research Project on Civil Aerospace Technology in Advance (D040301), the National Nature Science Foundation of China (61971157) and the Science Foundation of Aeronautics of China (201901077005).

REFERENCES

1. Venneri, F., S. Costanzo, and G. Di Massa, "Design and validation of a reconfigurable single varactor-tuned reflectarray," *IEEE Transactions on Antennas and Propagation*, Vol. 61, No. 2, 635–645, Feb. 2013.
2. Wu, F., R. Lu, J. Wang, Z. H. Jiang, W. Hong, and K.-M. Luk, "Circularly polarized one-bit reconfigurable ME-dipole reflectarray at X-band," *IEEE Antennas and Wireless Propagation Letters*, Vol. 21, No. 3, 496–500, Mar. 2022.
3. Wu, F., R. Lu, J. Wang, Z. H. Jiang, W. Hong, and K.-M. Luk, "A circularly polarized 1 bit electronically reconfigurable reflectarray based on electromagnetic element rotation," *IEEE Transactions on Antennas and Propagation*, Vol. 69, No. 9, 5585–5595, Sept. 2021.
4. Wang, Z., "1 bit electronically reconfigurable folded reflectarray antenna based on p-i-n diodes for wide-angle beam-scanning applications," *IEEE Transactions on Antennas and Propagation*, Vol. 68, No. 9, 6806–6810, Sept. 2020.
5. Baladi, E., M. Y. Xu, N. Faria, J. Nicholls, and S. V. Hum, "Dual-band circularly polarized fully reconfigurable reflectarray antenna for satellite applications in the Ku-band," *IEEE Transactions on Antennas and Propagation*, Vol. 69, No. 12, 8387–8396, Dec. 2021.
6. Han, J., L. Li, G. Liu, Z. Wu, and Y. Shi, "A wideband 1 bit 12×12 reconfigurable beam-scanning reflectarray: Design, fabrication, and measurement," *IEEE Antennas and Wireless Propagation Letters*, Vol. 18, No. 6, 1268–1272, Jun. 2019.
7. Luo, C.-W., G. Zhao, Y.-C. Jiao, G.-T. Chen, and Y.-D. Yan, "Wideband 1 bit reconfigurable transmitarray antenna based on polarization rotation element," *IEEE Antennas and Wireless Propagation Letters*, Vol. 20, No. 5, 798–802, May 2021.
8. Clemente, A., L. Dussopt, R. Sauleau, P. Potier, and P. Pouliguen, "Wideband 400-element electronically reconfigurable transmitarray in X band," *IEEE Transactions on Antennas and Propagation*, Vol. 61, No. 10, 5017–5027, Oct. 2013.
9. Nguyen, B. D. and C. Pichot, "Unit-cell loaded with PIN diodes for 1-bit linearly polarized reconfigurable transmitarrays," *IEEE Antennas and Wireless Propagation Letters*, Vol. 18, No. 1, 98–102, Jan. 2019.
10. Li, H., "Reconfigurable fresnel lens based on an active second-order bandpass frequency-selective surface," *IEEE Transactions on Antennas and Propagation*, Vol. 68, No. 5, 4054–4059, May 2020.
11. Liu, G. Y., L. Li, J. Q. Han, H. X. Liu, X. H. Gao, Y. Shi, and T. J. Cui, "Frequency-domain and spatial-domain reconfigurable metasurface," *ACS Applied Materials and Interfaces*, Vol. 12, No. 20, 23554–23564, Dec. 2020.
12. Lau, J. Y. and S. V. Hum, "A wideband reconfigurable transmitarray element," *IEEE Transactions on Antennas and Propagation*, Vol. 60, No. 3, 1303–1311, Mar. 2012.
13. Huang, C., W. Pan, and X. Luo, "Low-loss circularly polarized transmitarray for beam steering application," *IEEE Transactions on Antennas and Propagation*, Vol. 64, No. 10, 4471–4476, Oct. 2016.
14. Yang, H., F. Yang, S. Xu, M. Li, X. Cao, and J. Gao, "A 1-bit multipolarization reflectarray element for reconfigurable large-aperture antennas," *IEEE Antennas and Wireless Propagation Letters*, Vol. 16, 581–584, 2017.
15. Xu, H., S. Xu, F. Yang, and M. Li, "Design and experiment of a dual-band 1 bit reconfigurable reflectarray antenna with independent large-angle beam scanning capability," *IEEE Antennas and Wireless Propagation Letters*, Vol. 19, No. 11, 1896–1900, Nov. 2020.

16. Zhou, S.-G., "A wideband 1-bit reconfigurable reflectarray antenna at Ku-band," *IEEE Antennas and Wireless Propagation Letters*, Vol. 21, 566–570, Mar. 2022.
17. Diaby, F., A. Clemente, R. Sauleau, K. T. Pham, and L. Dussopt, "2 bit reconfigurable unit-cell and electronically steerable transmitarray at Ka-band," *IEEE Transactions on Antennas and Propagation*, Vol. 68, No. 6, 5003–5008, Jun. 2020.
18. Clemente, A., F. Diaby, L. D. Palma, L. Dussopt, and R. Sauleau, "Experimental validation of a 2-bit reconfigurable unit-cell for transmitarrays at Ka-band," *IEEE Access*, Vol. 8, 114991–114997, 2020.
19. Yu, J., W. Jiang, and S. Gong, "Design of a 2.5-D 2-bit reconfigurable transmitarray element for 5G mmWave applications," *IEEE Antennas and Wireless Propagation Letters*, Vol. 18, No. 10, 2016–2020, Oct. 2019.
20. Theofanopoulos, P. C. and G. C. Trichopoulos, "A novel 2-bit graphene reconfigurable reflectarray," *2020 IEEE International Symposium on Antennas and Propagation and North American Radio Science Meeting*, 1701–1702, 2020.
21. Li, S., F. Xu, X. Wan, T. J. Cui, and Y.-Q. Jin, "Programmable metasurface based on substrate-integrated waveguide for compact dynamic-pattern antenna," *IEEE Transactions on Antennas and Propagation*, Vol. 69, No. 5, 2958–2962, May 2021.
22. Luo, Y., K. Qin, H. Ke, B. Xu, S. Xu, and G. Yang, "Active metamaterial antenna with beam scanning manipulation based on a digitally modulated array factor method," *IEEE Transactions on Antennas and Propagation*, Vol. 69, No. 2, 1198–1203, Feb. 2021.
23. Ji, L., Z. Zhang, and N. Liu, "A two-dimensional beam-steering partially reflective surface (PRS) antenna using a reconfigurable FSS structure," *IEEE Antennas and Wireless Propagation Letters*, Vol. 18, No. 6, 1076–1080, Jun. 2019.
24. Liu, P., Y. Li, and Z. Zhang, "Circularly polarized 2 bit reconfigurable beam-steering antenna array," *IEEE Transactions on Antennas and Propagation*, Vol. 68, No. 3, 2416–2421, Mar. 2020.
25. Hu, J., Y. Li, and Z. Zhang, "A novel reconfigurable miniaturized phase shifter for 2-D beam steering 2-bit array applications," *IEEE Antennas and Wireless Propagation Letters*, Vol. 31, No. 4, 381–384, Apr. 2021.
26. Mailloux, R. J., *Phased Array Antenna Handbook*, 2nd Edition, Artech House, Norwood, MA, USA, 2005.